Structural Modeling of Aircraft Tires

S. K. CLARK,* R. N. DODGE,† J. I. LACKEY,‡ AND G. H. NYBAKKEN‡
University of Michigan, Ann Arbor, Mich.

A research program has investigated the problem of producing small scale models of aircraft tires. It has been shown that such a scaling can be obtained in theory for the mechanical properties of aircraft tires, both static and dynamic, as well as for the over-all or macroscopic stress state of such tires but not for their detailed or microscopic stress state. The question of thermal modeling is still unresolved but theoretical indications are that tire temperature distributions will not be similar or analogous between model and prototype. Experiments have been conducted on a small scale model of a 40 × 12, 14 PR, Type VII aircraft tire, with a scaling factor of 8.65. Agreement is excellent between the basic static tire mechanical characteristics in model and prototype, referred to a dimensionless basis. The structural modeling concept discussed in this paper is believed to be exact for mechanical properties of an aircraft tire, including static, rolling, and transient conditions.

Nomenclature

C = couple or moment on tire
c_p = specific heat of tire material
D = tire nominal diameter
E = tire carcass modulus of elasticity
F = load on tire
h = heat-transfer coefficient between tire and surrounding air
K = thermal conductivity of tire material
k_o = radius of gyration of tire about its axis of rotation
k_x, k_y, k_z = tire elastic stiffness, or spring rates
L = length
M = mass
p_o = tire inflation pressure
T = time
V = wheel forward velocity
w = tire section width
δ = tire deflection
θ = temperature
λ = tire relaxation length
μ = Poisson's ratio of tire materials
Π = dimensionless factors
ρ = tire material density
σ = tire stress
ψ = angle of rotation of tire about a vertical, or steer, axis

Subscripts

m = model
p = prototype
x, y, z = coordinate directions according to Fig. 2

Introduction

THE measurement of mechanical properties of aircraft tires is an expensive and lengthy process. Aircraft tires normally tend to be rather heavily loaded as compared with conventional automobile and truck tires, and to be run at quite high speeds, so the equipment to simulate field operating conditions is large and expensive. Only one major facility exists in the United States for the controlled study of aircraft tire characteristics under landing conditions. This is the well-known Landing Loads Simulator Track at NASA, Langley Field, Va.

One possible solution to the difficulty of obtaining full size aircraft tire mechanical data is to generate such data on small scale models. This has the advantage of allowing the necessary measurements to be made much more quickly and economically. It also allows measurements of aircraft tire properties under extreme conditions, which cannot be tolerated on full scale experiments for safety reasons.

Theory of Modeling

The theory of tire modeling may be divided into three separate categories or sets of modeling requirements, involving tire mechanical properties, tire stresses and tire temperatures. These will be discussed separately.

Modeling of Tire Mechanical Properties

The first, and least restrictive case, is modeling of tire mechanical properties, which is the primary concern of this paper. For that purpose, consider the tire mechanical properties, both static and dynamic, to be defined by the engineering variables illustrated in Fig. 1.

It should be noted that the tire carcass properties are represented as single quantities E and μ, although in reality they are distributions of elastic properties throughout the carcass. This dimensionless distribution must be maintained in the model tire exactly as in the full-size tire in order for modeling to be exact. This is a requirement which is analogous to the need for geometric similarity between model and prototype, a well-known and universally accepted condition.

Several obvious dimensionless variables may be identified by inspection. These are

Π_1 = complete geometric similarity between model and prototype, including the dimensionless distribution of elastic properties between model and prototype for the tire carcass (1)

$$\Pi_2 = \delta/D \quad (2)$$

$$\Pi_3 = k_o/D \quad (3)$$

$$\Pi_4 = p_o/E \quad (4)$$

$$\Pi_5 = \mu \quad (5)$$

$$\Pi_6 = FD/C \quad (6)$$

Received March 31, 1971; presented as Paper 71-346 at the AIAA/ASME 12th Structures, Structural Dynamics and Materials Conference, Anaheim, Calif., April 19–21, 1971; revision received, October 18, 1971. This work was supported by NASA Langley Research Center, under Grant NGL 23-005-010.

Index category: Aircraft Landing Dynamics.

* Professor of Engineering Mechanics and Mechanical Engineering.

† Research Assistant, Engineering Mechanics.

‡ Graduate Student, Engineering Mechanics.

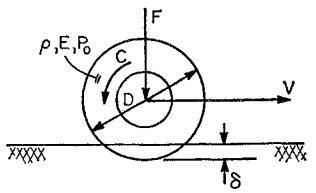

Fig. 1 Tire geometry and nomenclature.

The remaining terms may be written in a general functional relation using a typical dependent property, the relaxation length λ of the tire. One may express this as a function of the pertinent engineering variables remaining as

$$(\lambda/D) = f(F, \langle 6 \rangle V, p_o, D, \rho) \tag{7}$$

The method used to obtain the dimensionless variables from a relationship such as Eq. (7) is taken from Langhaar.[1] From this, one obtains two additional Π terms which must be held constant in order that the model and prototype are identical

$$\Pi_7 = (F/p_o D^2) \quad \Pi_8 = (V^2\rho/p_o) = (V^2\rho/E) \quad \text{using } \Pi_4 \tag{8}$$

Of these terms Π_8 is the ratio of tire velocity to a characteristic wave velocity, and is similar in concept to a Mach number. Π_7 is, however, the important scaling parameter since it relates the tire inflation pressure p_o, tire diameter D and force F acting on the tire, between model and prototype. In view of the fact that complete geometric similarity is an additional requirement, then any appropriate tire section width, tire diameter, or tire section height could be used in place of the diameter D in Π_7 so long as the dimensional character of that term remains the same. R. K. Gordon[2] has arrived at Π_7 by a somewhat different line of reasoning.

A short discussion of the scaling parameter Π_7 is in order. If the inflation pressures for model and prototype are known, and if the relative sizes of model and prototype are known, then the appropriate forces for model and prototype may be determined by the fact that Π_7 must be equal for model and prototype in a given test situation. The scale ratio or model diameter D is at the choice of the experimenter. The pressure p_o must, however, be determined in conjunction with the required equality for Π_4. This latter term demands that the ratio of inflation pressure of the model tire to its modulus of elasticity must be identical to that ratio in the full-size prototype. Under those conditions, it may be seen that one may construct the small model of a large aircraft tire using a purposely lower modulus of elasticity in the model. This will allow a lower inflation pressure p_o, since in the model the ratio (p_o/E) must remain the same as in the prototype. This further means that in evaluating the dimensionless term Π_8, the influence of velocity of travel will be amplified in the model. For example, if in the model it is possible to use a low modulus of elasticity and a relatively low pressure, reference to Eq. (8) shows that the model velocity can be made significantly higher. This is seen by equating Π_8 for the model and prototype, and solving for the model velocity. This gives

$$V_m = (E_m/E_p)^{1/2}(\rho_p/\rho_m)^{1/2} V_p \tag{9}$$

where the subscripts m and p refer to model and prototype, respectively.

If the material densities of the prototype and model are essentially the same, Eq. (9) shows that the model velocity V_m needed to obtain an equivalent prototype velocity V_p may be substantially less than the prototype velocity by the ratio of the square root of the model tire modulus to the prototype modulus. Methods of controlling tire modulus are available and may be used to advantage here. In effect, high-speed tire testing on the model can be conducted at relatively low speeds.

In general, this dimensional analysis shows that a typical tire response quantity relaxation length λ is related to the dimensionless Π terms through the relationship

$$\lambda/D = f(\Pi_1, \Pi_2, \ldots \Pi_8) \tag{10}$$

From this, it may be concluded that tire mechanical properties may be readily modeled between full-size tire and small scale tire provided that one learns how to use tire materials in such a way that the distribution of carcass stiffness or elastic constants is the same between model and prototype, and that preferably the absolute level of the elastic constants be significantly reduced in the model compared to the prototype, without changing the relative or dimensionless distribution.

Modeling of Tire Stress Levels

A second level of sophistication in tire modeling theory may be brought about by attempting to model the internal stress state between scale model and prototype, in addition to the appropriate mechanical properties. Assume that the tire stress is governed by the same engineering variables as shown in Fig. 1, where all symbols are the same as before except for the stress level σ.

It is recognized from the previous dimensional analysis that six dimensionless products Π_1 through Π_6 must be automatically satisfied by any model. Assuming these to be true, the stress state in the moving tire may now be expressed in the general functional form

$$\sigma/p_o = f(p_o, D, F, \rho) \tag{11}$$

The right-hand side of Eq. (11) is identical to that of Eq. (7), so that the dimensionless quantities governing this are identical to those previously gotten in Eq. (8), i.e.

$$\Pi_7 = F/p_o D^2 \tag{12}$$

$$\Pi_8 = V^2\rho/E \tag{13}$$

Now one may write

$$\sigma = p_o f(\Pi_1, \Pi_2, \ldots \Pi_8) \tag{14}$$

Equation (14) shows that if one wishes to maintain the same stress level in model and prototype, then all terms Π_1,–Π_8 must be held identical, and in addition the inflation pressure p_o must be the same in both model and full-size tire. Since p_o must be constant, then from Π_4 [Eq. (4)] it is seen that modulus of elasticity E of both model and full-size tire must also be the same. In effect, this forces one to use the same materials for the model as the full-size tire.

It should be noted that this set of requirements is somewhat more restrictive than the previous set which dealt with mechanical properties of the tire alone. Here, the pressure is specified as is the modulus of elasticity of the model tire material. This was not the case in the previous analysis describing only mechanical properties, where it was possible to reduce modulus and pressure simultaneously and still retain dimensional similarity. This simply means that in the previous case, the stress levels in the model tire were not equal to those in the prototype. Here, where equal stress levels are desired, the additional restrictions of pressure and modulus equality are necessary.

In order that this situation be understood more clearly, it should be mentioned that in a practical sense it is essentially impossible to insure that a textile-cord structure be made in small scale that is identical in all respects to a similar structure in large size. Textile cords are manufactured only in discrete sizes and in general cannot be scaled downward arbitrarily. The details of aircraft tire construction are sometimes so numerous as to render the construction of a completely similar small model almost impossible, even though the over all, macroscopic constants of the tire carcass material may be successfully modeled. For these reasons it is very probable

that such effects as durability and failure will be very difficult to assess on a scale model with any significant scale ratio simply due to the basic unavailability of the proper materials, and the great difficulty of producing a completely geometrically similar structure.

In the event that such tire stress comparisons are desired, it should again be emphasized that the modulus of elasticity, or elastic constants, of the model and full-size tire must be held the same, that the inflation pressure of the model must be identical to that of the prototype, and that the surface speeds must also be equal between the two. Under these conditions, forces proportional to the square of the scale factor arise between model and prototype, as indicated by Eq. (12), while the over all or macroscopic internal stress state of the model tire is the same as the full-size tire.

Modeling of Tire Equilibrium Temperature

Now consider the somewhat more complex case of including in the analysis the quantities which determine the equilibrium temperature of the running tire. In order to do this, we adopt Eq. (15) as a basic statement of functional dependence.

$$K\theta/\rho V^3 D = f(p_o, D, V, F, \rho, c_p, K, h) \tag{15}$$

The particular form of the left-hand side of Eq. (15) is chosen so as to represent temperature in a dimensionless fashion. Other representations are possible, but do not lead to anything different.

A dimensional analysis of these variables leads to the following dimensionless characteristics which must be equal between model and prototype, over and above those given by Eqs. (5–14), previously derived

$$\Pi_7 = K/Dh \tag{16}$$

$$\Pi_8 = h/V \cdot \rho \cdot c_p \tag{17}$$

Of these two dimensionless quantities, Eq. (17) will be automatically satisfied provided that the conditions described in the previous dimensionless analysis are fulfilled, that is, the velocity of running and density of the tire material are the same between model and prototype. This is because the heat-transfer coefficient h and the material specific heat c_p will be approximately the same in the full-size tire as in the model.

However, Π_7 very probably will not be equal between model and prototype, since the heat-transfer coefficient h and thermal conductivity K of both model and full-size tires will be approximately the same, whereas the characteristic length D will vary as the scale factor. Based on this, Eq. (15) may be rewritten as

$$\theta = V^2/c_p f(\Pi_1, \Pi_2, \Pi_3, \Pi_4, \Pi_5, \Pi_6, \Pi_7, \Pi_8) \tag{18}$$

From this, it may be seen that the temperature θ of the model tire will be the same as that of the prototype provided that the velocity of travel and the specific heat of the tire material are the same as in the full size tire, and in addition that all of the dimensionless factors Π_1–Π_8 are held constant between the scale model and the full-size tire. As was just discussed, it is possible to do this with the exception of the single dimensionless factor Π_7. Its influence on the equilibrium temperature is not known but may be substantial, since in effect it represents the ratio between the volume of the tire which generates heat and the convective heat transfer surface area of the tire. It is possible under particularly fortuitous conditions that a good approximation to the full-size temperature may be obtained from a model tire, but it appears that no automatic guarantee of this exists. Therefore, it is concluded that in general thermal modeling of aircraft tire temperature rise may not be possible without extensive experimentation and the development of suitable scaling factors based on experimental data.

Mechanical Properties of Model and Prototype Tires

From the previous discussion on modeling, it is seen that certain dimensionless variables must be the same for model and prototype. This necessitates measurement of such quantities on both tires. Full-size tire data is scarce so that the tire selection must be based on available prototype data. Here the earlier work of Smiley and Horne[3] is used as a source for data on the 40 × 12 14 PR Type VII aircraft tire. Scale models of this tire were built to an 8.65:1 scale ratio. The model tires were constructed carefully to assure geometric similarity. The cord content was scaled by reducing the total cord end-count of the tire cross section, rather than scaling the individual cord diameter. To simplify tire construction, beadless tires were designed which gave the correct tire section when mounted. Four such model tires were tested for these results.

The tire co-ordinate system used in this work is shown in Fig. 2. The slow rolling properties quoted later are based on the ψ direction normal to the wheel plane, which reduces to the y direction for an unyawed tire.

Ten dimensionless properties were chosen for comparison of model and prototype. These ten represent basic static tire stiffness data as well as tire properties commonly used in shimmy analysis. It was felt that good agreement between model and prototype in these ten properties would be a strong indication of the validity of tire modeling. These ten properties are listed below. The static properties are: 1) fore-aft load deflection F_x vs δ_x, 2) lateral load-deflection F_y vs δ_y, 3) lateral damping η_y, 4) vertical load-deflection F_z vs δ_z, 5) twisting moment-rotation C_z vs ψ, and 6) footprint half-length ℓ.

The slow rolling properties are: 7) relaxation length λ, 8) side force-yaw angle F_ψ vs ψ, 9) self-aligning torque-yaw angle C_z vs ψ, and 10) pneumatic trail-yaw angle q vs ψ.

The dimensionless number (E/p_o) can only be found by measuring tire carcass effective modulus. This measurement of E of the tire is difficult unless it is recognized that the measurement of fore-aft stiffness k_x is in a gross over-all sense, a measure of the tire elastic modulus E. The assumption that fore-aft stiffness is almost entirely a carcass elasticity effect is thought to be valid since this stiffness is known to be relatively independent of inflation pressure near the rated inflation pressure. Assuming k_x to be proportional to E, then

$$p_o/E \sim p_o/k_x$$

Then knowing the appropriate full-size tire data, and knowing D and k_x for the model, the dimensionless parameters F_x/p_oD^2 and δ_x/D can be manipulated to give the rated inflation pressure of the model, as well as the rated vertical load. First the equation

$$(p_o)_m = (k_x/D)_m(D/k_x)_p(p_o)_p \tag{19}$$

is used to find inflation pressure and then

$$(F_z)_m = (F_z)_p(p_oD^2)_m/(p_oD^2)_p \tag{20}$$

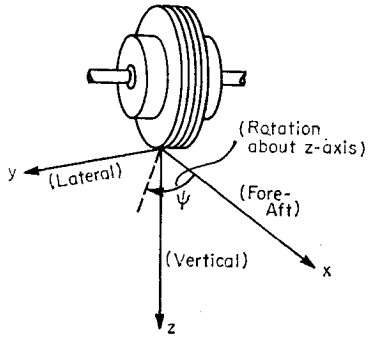

Fig. 2 Tire co-ordinate directions.

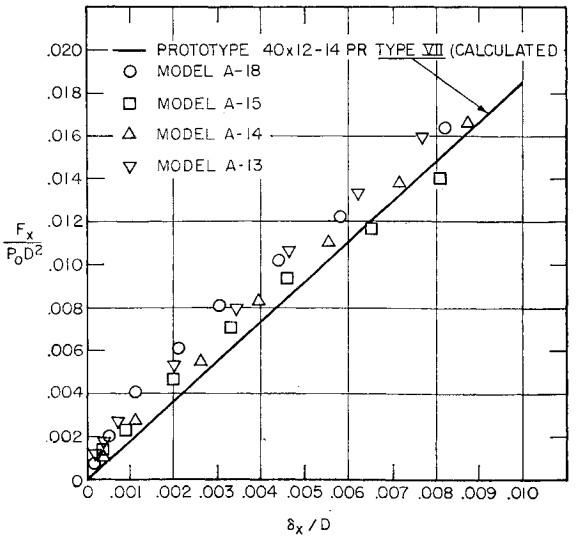

Fig. 3 Fore-aft load-deflection data for model and prototype tires.

Table 1 Tire operating conditions

Tire	p_o psi	F_z lb	D, in.	w^a in.
40 × 12 — 14 PR Type VII Prototype	95	14500	39.3	12.12
Model A-18 (2 Ply, 840/2 Nylon, 10 EPI)	25	48.2	4.57	1.67
Model A-15 (2 Ply, 840/2 Nylon, 10 EPI)	23	48.2	4.58	1.66
Model A-14 (2 Ply, 840/2 Nylon, 10 EPI)	19	38.2	4.58	1.64
Model A-13 (2 Ply, 840/2 Nylon, 10 EPI)	20	38.2	4.56	1.62

[a] w = Section width.

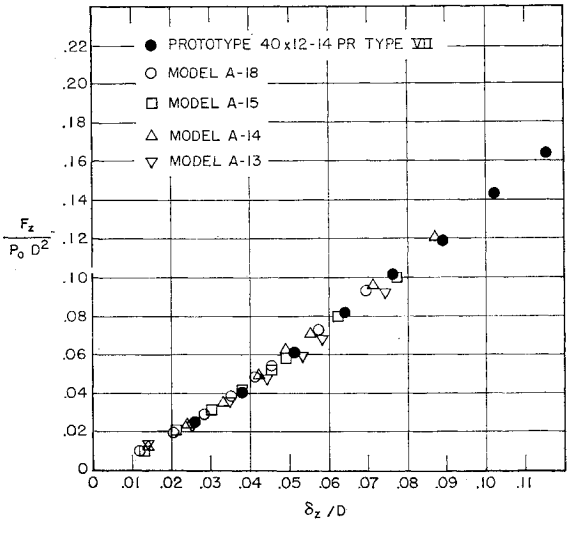

Fig. 4 Vertical load-vertical deflection data for model and prototype tires.

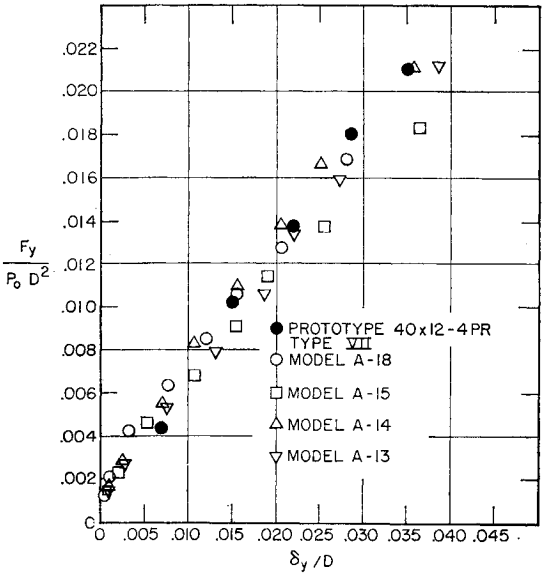

Fig. 5 Lateral load-lateral deflection data for model and prototype tires.

gives the vertical load, where $(F_z)_p$ is the rated load for the tire. Thus, this procedure forces the dimensionless plot of fore-aft data for model and prototype to coincide, since one has been used to define the other. Figure 3 shows this data with the prototype indicated by the solid line. Although the slopes were forced to be the same, this figure gives a good indication of data scatter. Table 1 shows the prototype and model tire operating conditions determined by this method.

The standard conditions of vertical load and inflation pressure generated by this procedure were used in all other tests. These other load-deflection plots are shown in Figs. 4–6. Here the prototype data is shown as well as the data for the four models. Agreement is satisfactory in all cases.

Lateral damping is defined by Smiley and Horne as the ratio of maximum half-height of the corresponding force-

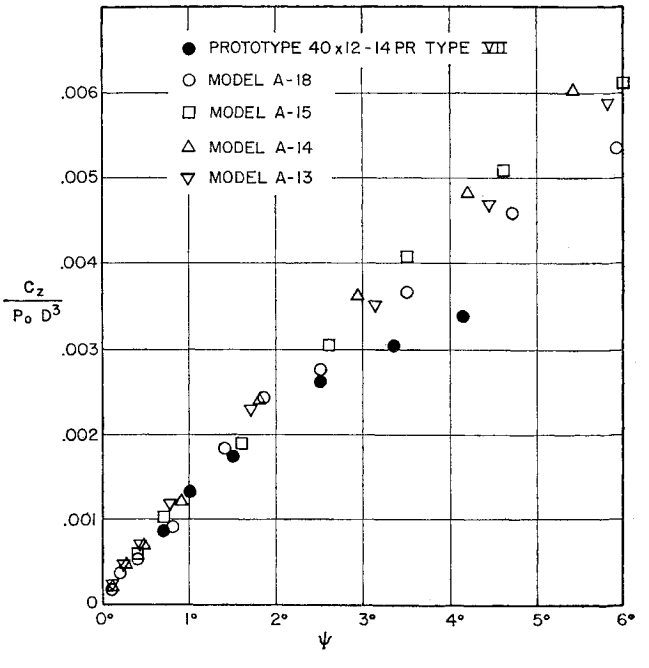

Fig. 6 Twisting moment-rotation data for model and prototype tires.

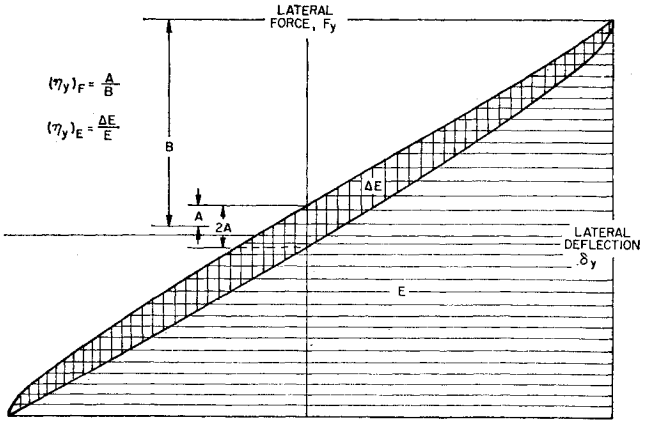

Fig. 7 Typical lateral hysteresis curve.

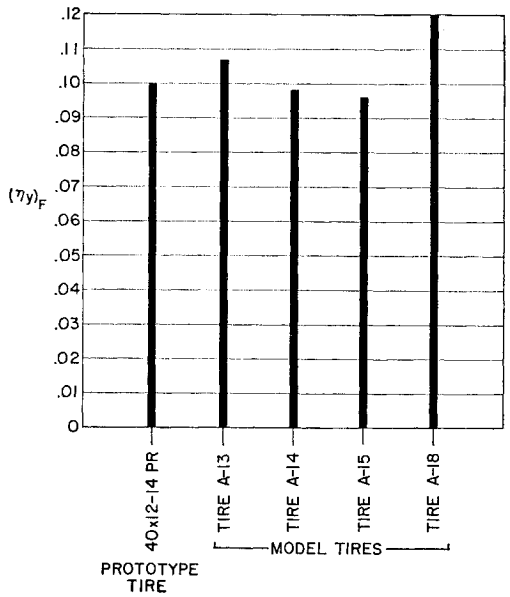

Fig. 8 Lateral damping coefficient data for model and prototype tires, $(\eta_y)_F$ based on force ratio.

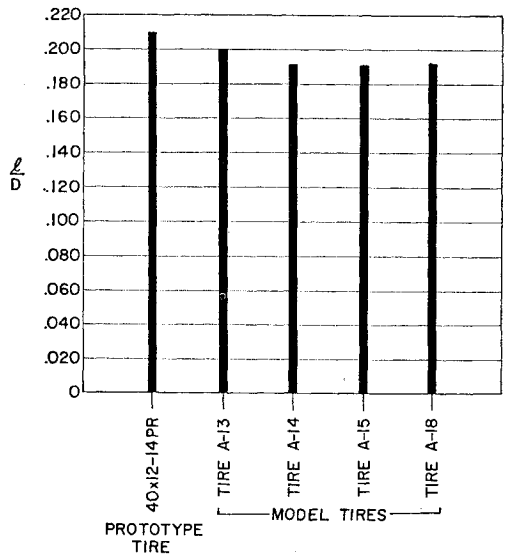

Fig. 9 Tire half contact-patch length data for model and prototype tires.

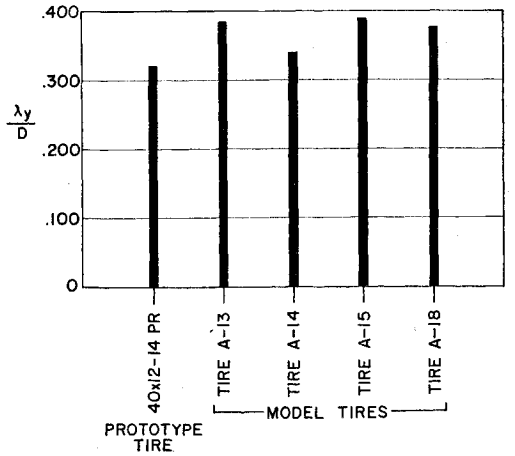

Fig. 10 Yawed-rolling relaxation length data for model and prototype tires.

deflection hysteresis loop to the maximum total force, that is, the ratio A/B in Fig. 7.

Figure 8 gives the comparison between model and prototype damping. Definitions of damping based on area quantities give similar results. Half-contact length data is illustrated in Fig. 9. Here again agreement is satisfactory.

At this point it should be noted that these model tires had been exercised on a small road wheel prior to testing. This procedure results in stable mechanical properties as has been recognized by tire manufacturers and testers for some time.

The slow rolling properties were tested on this same road wheel. Relaxation length data was derived from the side force

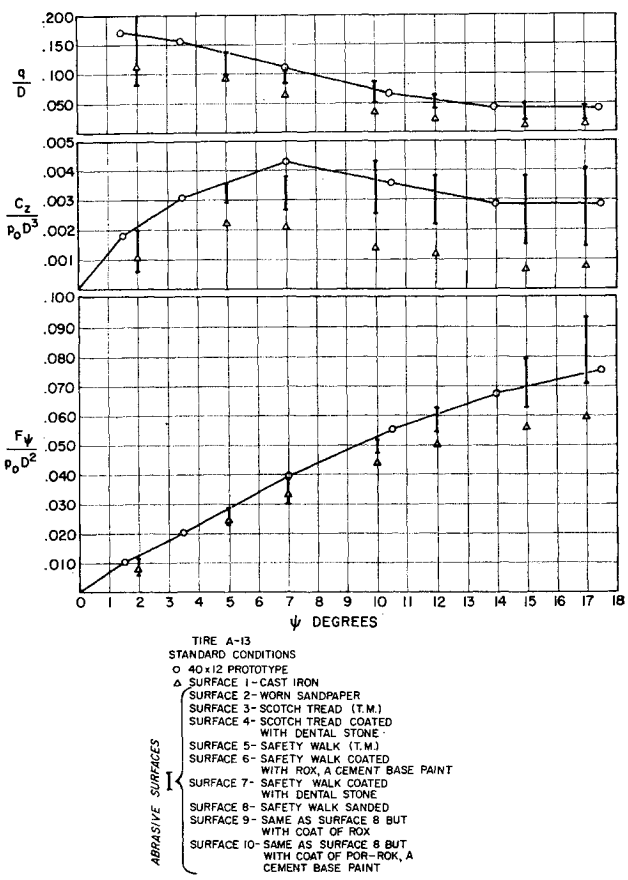

Fig. 11 Side force, self-aligning torque and pneumatic trial data for model and prototype tires.

build-up of a yawed tire. The relaxation length is defined as the distance the tire rolls, after one contact length, to achieve a side force of $e^{-1} \cdot A$, where A is the maximum side force attained in the steady state at that yaw angle. The yaw angle of 3.5° used by Smiley and Horne[3] was also used in obtaining the data shown in Fig. 10. Again the comparison is good.

The last three properties are derived from the steady-state values of side force F_ψ, and self-aligning torque C_z. Pneumatic trail is defined as their ratio, $q = C_z/F_\psi$. These properties are quite dependent on road wheel friction, and results using a number of surfaces are presented in Fig. 11, along with the original prototype data taken on a concrete runway. Here the results show some scatter, in great part due to frictional influences but also due to the model tire data being taken on a curved road wheel, while the prototype was taken on the flat runway surface. This means that contact pressure distributions were different, and that some variations in self aligning torque are certain to occur.

Measurement of Tire Mechanical Properties

Experimental reproducibility was excellent for the data obtained from the four model tires used here. Vertical load deflection data could be reproduced within $\pm 3\%$, twisting data within $\pm 8\%$, with lateral and fore-aft stiffness data to within $\pm 10\%$. To compensate for these variations, averages were taken of three different measurements at various circumferential locations around the tire.

Slow rolling mechanical tests were run on a four inch wide, 30 in. diameter cast iron road wheel which could be moved at a relatively slow speed, approximately 1 fps. The tire and rim assembly was mounted on a yoke attached to a hinged arm, on which various levels of deadweight could be loaded. This is shown in Fig. 12. Small transducers were installed to measure self-aligning torque about the vertical steer axis, as well as side force in the yawed tire. Using these force transducers, it was possible to measure relaxation length, side force and self-aligning torque for a given steer angle. From the latter two pieces of information, the pneumatic trail could be determined by calculation.

As previously mentioned, the steady-state average values of side force and self-aligning torque are quite dependent upon the particular friction characteristics of the surface against which the tire runs. Sharp, abrasive surfaces on the road wheel tend to give higher values of both side force and self-aligning torque, especially at yaw angles below 10°. These surfaces, however, tend to severely abrade the tires and must be used with caution. A number of different surfaces were investigated for purposes of determining the influence of surface characteristics on these particular mechanical properties. As previously pointed out and as illustrated in Fig. 11, a substantial variation in these mechanical properties is caused by different friction surfaces.

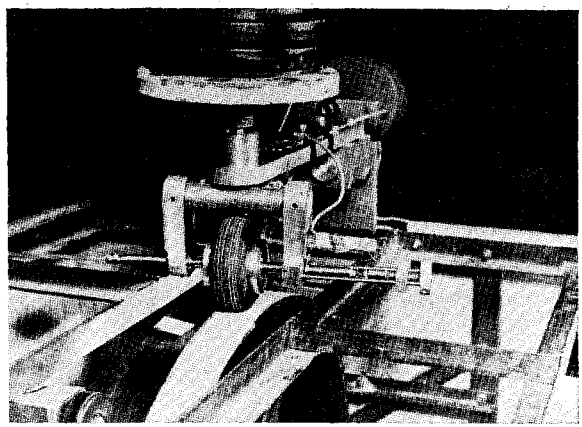

Fig. 12 Measurement of side force characteristics of model tire on road-wheel.

Conclusions

It is concluded from the data presented here that the concept of small scale modeling of the mechanical properties of aircraft tires is both theoretically and practically achievable. Based on this conclusion, it is felt that aircraft tire mechanical property data is more easily obtained by scale modeling, coupled with judicious selected full scale experiments, than by any other method.

References

[1] Langhaar, H. L., "Dimensional Analysis and Theory of Models," Wiley, New York, 1951.

[2] Gordon, R. K., "Modeling of Tires." *Soviet Rubber Technology*, Vol. 24 No. 6, 1965, p. 30.

[3] Horne, W. B. and Smiley, R. F., "Low Speed Yawed Rolling Characteristics and Other Elastic Properties of a Pair of 40 Inch Diameter 14 Ply Rating Type VII Aircraft Tires," 4109, Washington, D. C., Jan. 1958, NACA.